

# Coercivity of magnetic domain wall motion near the edge of a terrace

Cite as: Journal of Applied Physics **78**, 380 (1995); <https://doi.org/10.1063/1.360611>

Submitted: 12 September 1994 . Accepted: 14 March 1995 . Published Online: 04 June 1998

Yung-Chieh Hsieh, and M. Mansuripur



View Online



Export Citation

## ARTICLES YOU MAY BE INTERESTED IN

[Magnetic multilayers on porous anodized alumina for percolated perpendicular media](#)  
Applied Physics Letters **91**, 132505 (2007); <https://doi.org/10.1063/1.2790788>

### Ultra High Performance SDD Detectors



See all our XRF Solutions

# Coercivity of magnetic domain wall motion near the edge of a terrace

Yung-Chieh Hsieh<sup>a)</sup> and M. Mansuripur

*Optical Sciences Center, University of Arizona, Tucson, Arizona 85721*

(Received 12 September 1994; accepted for publication 14 March 1995)

Domain wall motion near the edges of terraces (e.g., grooves, pits, plateaus, etc.) is studied using analytical techniques based on the minimum energy principle and computer simulations based on the dynamic Landau–Lifshitz–Gilbert equation. One-dimensional lattices of magnetic dipoles with variations either of the easy axis direction (corresponding to a tilt of the anisotropy axis at the edge) or of the nearest-neighbor exchange force (corresponding to a changing film thickness) are considered. We show that the coercivity caused by the terrace edge could be as large as several kilo Oe. © 1995 American Institute of Physics.

## I. INTRODUCTION

In magneto-optical disks a thin magnetic film (typically an amorphous TbFeCo alloy) is deposited on a grooved substrate. The grooves are usually *V*-shaped depressions on the otherwise flat surface of the substrate, having a depth of  $\sim 70$  nm and a width of about  $0.5 \mu\text{m}$ . The grooves are separated from each other by the so-called “land” regions, which have a width of about  $1 \mu\text{m}$ . The magnetic film is sputter-deposited on the grooved surface of the substrate, and has a thickness of  $\sim 30$  nm. Observations using polarized light microscopy have revealed that magnetic domains recorded on the land regions of the disk have a tendency to stick to the edges of the grooves and not propagate beyond these edges, unless a magnetic field with a relatively large amplitude is applied.<sup>1</sup> It appears as though the groove edge is acting as a pinning site for the magnetic domain wall.

Several mechanisms can be conceived for the pinning effect at the groove edge. One possibility is that the direction of magnetic anisotropy (i.e., the easy axis of magnetization for the TbFeCo film) on the land is different from that on the walls of the *V*-shaped groove. This might seem a reasonable assumption in light of the fact that the direction of film deposition on average is perpendicular to the land regions, but has a certain obliquity relative to the groove walls. Another possibility is that the film on the groove might be somewhat thinner than that on the land, causing the surface area of magnetic domain walls in the groove region to be smaller and, thereby, providing a low-energy environment (i.e., a potential well) for the domain walls. Yet a third possibility exists that the film composition (namely, the percentages of the rare earth and the transition metal in the alloy) may be different for the land and the groove regions. This seems plausible considering the fact that the resputtering rate of Terbium during film growth is known to be a function of the sputtering direction. If the composition happens to be close to the compensation composition at room temperature, then even a slight change of composition can cause a drastic change of coercivity, thereby creating a pinning effect at the edge of the groove. This effect, however, would be small when the average composition is far from the compensation

point and, moreover, its effect will depend on which side of the compensation composition the film happens to be: On one side of the compensation point, domains will stop when expanding from the land to the groove, while on the other side, having originated within the groove, they will stop when crossing over into the land. Based on numerous observations, however, we believe that the change of composition is not a determining factor of the pinning mechanism. We therefore consider the first two possibilities mentioned above as the likely causes of pinning, and set out to analyze them in this article.

Let us also mention that, in addition to explaining an observed phenomenon, the work in this area has been motivated by the possibility of utilizing the pinning effect to advantage in a somewhat different context. Suppose that the land regions on a magneto-optical disk substrate were embossed with regular depressions only a fraction of a micrometer across and a few nanometers deep. Then the writing and readout processes could be modified to take advantage of this patterned track by confining the domains within the depressions and by utilizing detection schemes (such as partial response) that are best suited to a jitter-free environment. We have recently demonstrated effective pinning of domains within square-shaped depressions that are only 20 nm deep, and are produced by ion-beam milling on a glass substrate.<sup>2,3</sup> This observation can potentially lead to higher-density data storage systems and, therefore, merits closer examination.

### A. Scope of the article

The theoretical analysis presented in the following sections confirms that either one of the postulated mechanisms, namely, the change of the easy axis or the change of film thickness on the side-walls (side walls are the slanted regions of the grooves), can result in domain wall pinning, provided that the width of the side wall is greater than the width of the magnetic domain wall. (In TbFeCo films, typical domain walls have a width of  $\sim 10$  nm.) The consequences of the change of direction of the anisotropy axis will be discussed in Sec. II, and the effects of a reduced film thickness at the sidewall will be considered in Sec. III. In addition to dynamic simulations described in Sec. III B, we consider the effects of a reduced film thickness from the view point of the minimum energy principle in Sec. III C, and derive a rela-

<sup>a)</sup>Electronic mail: ychsieh@soliton.physics.arizona.edu

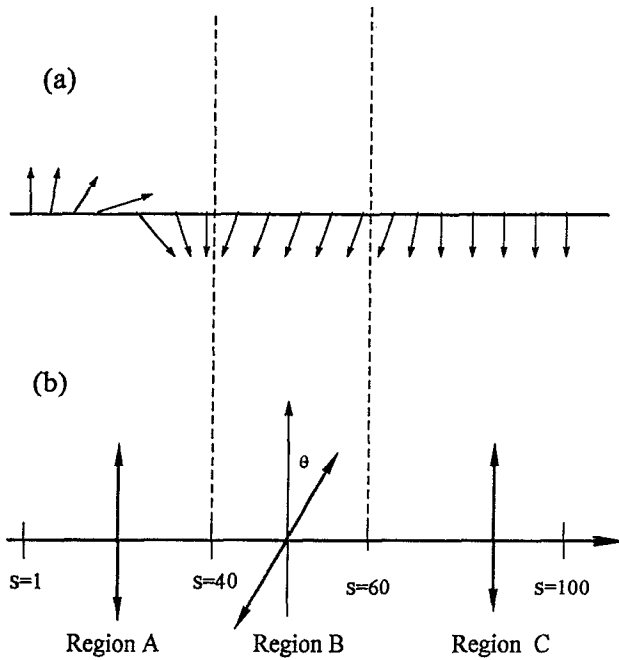


FIG. 1. (a) Schematic diagram showing magnetic dipoles in a one-dimensional lattice. A domain wall is shown centered in region A. In region B, the dipoles are not in the Z direction, but are tilted towards the easy axis. (b) Region B which contains lattice sites 40–60 has an easy axis tilted at angle  $\theta$  from the Z axis. Regions A and C have easy directions along the Z axis.

relationship between thickness variations and the coercivity of wall motion. It is not yet known which one of the two mechanisms is at work in real films, but the results of analysis and simulation are certainly consistent with the observations of numerous samples deposited on variously patterned substrates.

The simulations are based on the Landau–Lifshitz–Gilbert equation of magnetization dynamics. A system of one hundred dipoles in a one-dimensional lattice has been considered. Each dipole responds to an external magnetic field, interacts with its two nearest neighbors through exchange coupling, and also reacts to deviations from a local easy axis. For simplicity, the demagnetizing effects, which originate from classical, long-range dipole-dipole interactions, have been ignored.

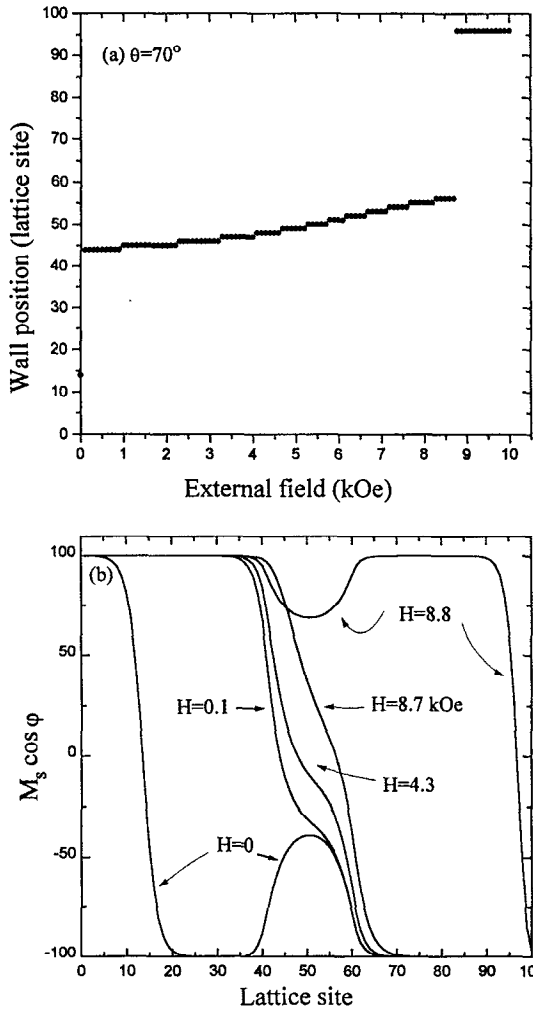
## II. TILT OF THE ANISOTROPY AXIS IN THE REGION OF THE SIDEWALL

The simulation is based on the methods described in Ref. 4. The following set of parameters was used throughout: saturation magnetization  $M_s = 100 \text{ emu/cm}^3$ , anisotropy constant  $K_u = 10^6 \text{ erg/cm}^3$ , macroscopic exchange stiffness coefficient  $A_x = 10^{-7} \text{ erg/cm}$ , gyromagnetic ratio  $\gamma = -10^7 \text{ Hz/Oe}$ , dipole spacing or lattice constant  $d = 10 \text{ \AA}$ , and viscous damping parameter  $\alpha = 3$ . The wall width parameter is thus given by  $\delta = (A_x/K_u)^{0.5} = 31.6 \text{ \AA}$ .

A one-dimensional array of magnetic dipoles containing a finite number of elements is shown in Fig. 1. We constrained the first dipole to have its moment oriented in the up direction, and the last dipole to have its moment in the down

direction. In regions A and C, the anisotropy axis is parallel to the Z axis. Region B, located on lattice sites from  $s = 40$  to  $s = 60$ , has an easy axis tilted away from the Z axis by an angle  $\theta$ . A domain wall placed in region A moves to region B under a small magnetic field,  $H_{\text{ext}}$ , applied in the positive Z direction. Upon increasing the external field gradually, we observe that the wall stays in the region B until the field reaches some critical value, at which point the wall leaves region B and enters region C. Figure 2(a) shows the dependence of the wall center position on the external field as obtained in one of our simulations for the case of  $\theta = 70^\circ$ . In the beginning, the wall center is at  $s = 14$ , but under an applied field of only 100 Oe, it moves to  $s = 44$ . Afterwards, the field increases, but the wall does not move substantially, staying in the vicinity of  $s = 50$ . When the applied field reaches 8.8 kOe, the wall suddenly jumps to  $s = 96$ . Figure 2(b) shows the wall shapes corresponding to several points in Fig. 2(a). The bump in the center region ( $s = 40\text{--}60$ ) for the curves corresponding to  $H = 0$  and  $H = 8.8 \text{ kOe}$  arises from the tilt of the anisotropy axis ( $\theta = 70^\circ$ ).

The physical reason for the observed behavior is as follows. The Landau–Lifshitz–Gilbert equation always pushes the system to a state of minimum energy. In the simulations, the total energy of the system consists of two parts: the magnetic domain wall energy and the external field energy, the wall energy being the sum of the anisotropy and exchange energies. Without an external field, the wall energy in regions A and C is equal to  $4(A_x K_u)^{1/2} = 1.26 \text{ erg/cm}^2$ . The external field energy density is equal to  $-MH \cos \phi$ , where  $\phi$  is the angle between magnetization and the direction of magnetic field. Therefore, with reference to Fig. 1, the external field exerts a driving force to move the wall to the right. Consider a situation where the anisotropy is uniform, with its axis pointing in the same direction everywhere. The wall energy is then independent of the wall position, but the external field energy decreases as the wall moves to the right. Therefore a fairly small field is all that is needed to move the wall. On the other hand, when region B has its easy axis tilted away from the Z axis, the anisotropy energy will be smaller if the wall stays in B rather than go to C. This is due to the fact that the average direction of the dipoles within the wall will be closer to the easy axis if the wall stays in B. Thus if the domain wall moves from B to C, its energy will increase. Only when the reduction in the external field energy is stronger than the rise in the wall energy, will the wall leave region B and enter C. Figure 2(c) shows plots of the anisotropy and exchange energies versus the iteration time for the simulation whose results were depicted in Figs. 2(a) and 2(b). The wall energy drops upon entering region B and stays low until the rising external field forces the wall out of the trap. [Note: The exchange and anisotropy energies plotted in Fig. 2(c) belong to the entire lattice and not just the domain wall. This is the reason why the exchange and anisotropy energies of the system, when the wall is located in either region A or C, add up to something greater than the  $1.26 \text{ erg/cm}^2$  value mentioned earlier. The extra energy is contained in region B and its borders with A and C.] Figure 3 shows the computed dependence of the critical field  $H_c$  on the angle  $\theta$  of the easy axis within region B of the lattice.



When  $\theta$  is close to zero, the critical field (i.e., the wall motion coercivity) is very nearly zero. The maximum value of the coercivity does not occur at  $\theta=90^\circ$ , as might perhaps have been expected, but at  $74^\circ$ .

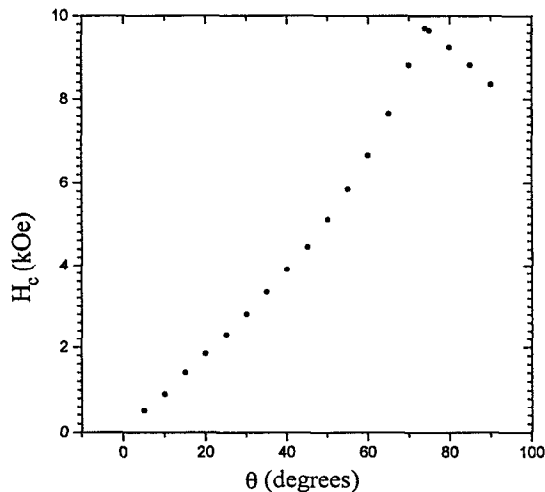


FIG. 3. Computed coercivity vs the deviation angle  $\theta$  of the easy axis in region B. The largest coercivity is seen to occur at  $\theta=74^\circ$ .

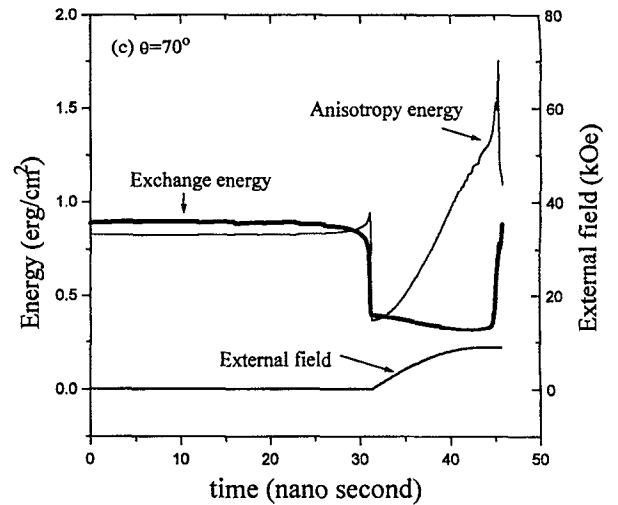


FIG. 2. (a) Computed position of the wall center versus the magnitude of the external field. The assumed deviation angle  $\theta$  of the anisotropy axis from the Z axis on the sidewall is  $70^\circ$ . The wall center, originally placed at  $s=14$ , moves to  $s=44$  with a 0.1 kOe field and stays in this vicinity until the field reaches 8.8 kOe. It then jumps to  $s=96$  and remains there afterwards. (b) Distribution of the Z component of magnetization  $M_z = M_s \cos \phi$  over the lattice, corresponding to several values of the external field. At  $H=0$  and  $H=8.8$  kOe, the orientation of dipoles within region B shows a clear tilt away from the Z axis. (c) Anisotropy and exchange energies of the lattice vs time during the movement of the domain wall from region A to region C. The bottom curve shows the corresponding variation of the external field. As long as the wall resides in region A, its anisotropy and exchange energies are fairly constant and nearly identical. Both energies are lowered when the wall arrives in region B. With the wall approaching the boundary between B and C, the anisotropy energy reaches a maximum. As the wall moves into region C, the energies revert to their original values.

### III. CHANGE OF FILM THICKNESS IN THE REGION OF THE SIDEWALL

#### A. Effective exchange field

Consider two adjacent cells of the lattice in the region of the magnetic film where the thickness is varying. These cells have volumes  $d^2h$  and  $d^2h_0$ , and magnetic moments  $\mathbf{m}$  and  $\mathbf{m}_0$ , as shown in Fig. 4. The exchange energy  $E_{\text{xchg}}$  for this pair of dipoles in the discrete approximation is

$$\begin{aligned}
 E_{\text{xchg}} &= \int A_x [(\nabla \alpha)^2 + (\nabla \beta)^2 + (\nabla \gamma)^2] d\nu \\
 &= \frac{2A_x}{d^2} \left( 1 - \frac{\mathbf{m} \cdot \mathbf{m}_0}{|\mathbf{m}| |\mathbf{m}_0|} \right) \left( \frac{h_0 + h}{2} \right) d^2 \\
 &= A_x (1 - \hat{\mathbf{m}} \cdot \hat{\mathbf{m}}_0) (h_0 + h), \quad (1)
 \end{aligned}$$

where  $\alpha, \beta, \gamma$  are the direction cosines of the magnetization and  $\hat{\mathbf{m}}$  denotes the unit vector. To derive an expression for the effective exchange field exerted on  $\mathbf{m}_0$  by  $\mathbf{m}$ , we keep  $\mathbf{m}$  fixed and rotate  $\mathbf{m}_0$  by a small angle. Then the exchange energy of the system has a variation corresponding to the change of the angle between  $\mathbf{m}$  and  $\mathbf{m}_0$ . The energy difference can be expressed in terms of either the effective field  $\mathbf{H}_{\text{eff}}$ , or the exchange stiffness coefficient:

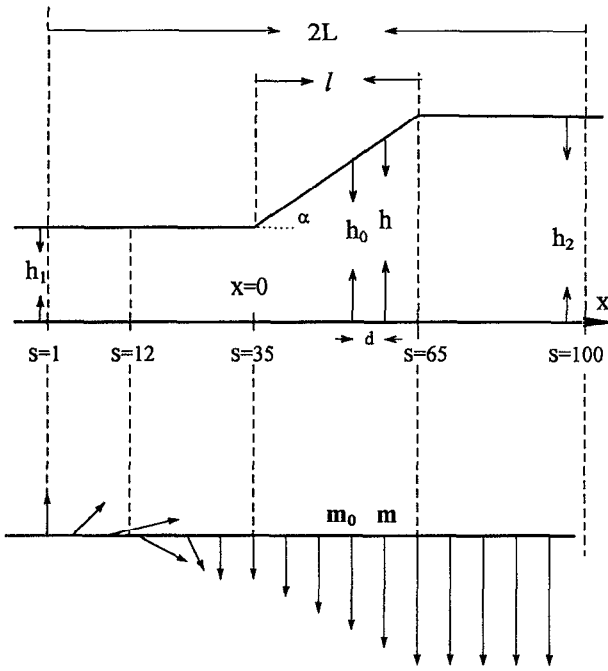


FIG. 4. Cross section of a film having variable thickness that changes from  $h_1$  to  $h_2$  with a slope given by  $\tan(\alpha)$ . Schematic diagram showing the simulated lattice of dipoles, with a linear dependence of the magnitude of the magnetic moments on the film thickness. The magnetic dipoles  $\mathbf{m}_0$  and  $\mathbf{m}$  correspond to two adjacent cells which have thicknesses  $h_0$  and  $h$ . The  $X$  axis denotes the direction along which the one-dimensional lattice of dipoles is defined with lattice constant  $d$ ;  $s$  denote the lattice sites. The 35th lattice site corresponds to  $x=0$ , and the film length  $2L$  is equal to  $100d$ .

$$\begin{aligned} \Delta E_{\text{exch}} &= -H_{\text{eff}} \cdot \Delta \mathbf{m}_0 = -H_{\text{eff}} \cdot \Delta \hat{m}_0 (M_s h_0 d^2) \\ &= -A_x (\hat{m} \cdot \Delta \hat{m}_0) (h + h_0). \end{aligned}$$

The effective exchange field may thus be written as follows:

$$H_{\text{eff}} = \frac{A_x}{M_s d^2} \left( \frac{h + h_0}{h_0} \right) \hat{m}. \quad (2)$$

This equation gives the exchange field in terms of the saturation magnetization  $M_s$ , local film thicknesses  $h_0$ ,  $h$ , and the lattice constant  $d$ .

## B. Simulation results

Consider a magnetic film whose thickness changes smoothly from  $h_1$  to  $h_2$  over a finite distance  $l$ , with a thickness gradient that we will denote by  $\tan(\alpha)$ . Figure 4 shows schematically the cross section of such a film, and a typical distribution of magnetic dipole moments within this cross section. In our simulation, the thickness changes gradually from  $h_1 = 150 \text{ \AA}$  at  $s = 35$  to  $h_2 = 450 \text{ \AA}$  at  $s = 65$ . Before  $s = 35$  and after  $s = 65$ , the thickness is uniform. The angle  $\alpha$  is equal to  $45^\circ$ . When a domain wall is placed at  $s = 12$ , it moves towards the corner at  $s = 35$  under an applied field of  $0.1 \text{ kOe}$ . Upon increasing the strength of the field, the wall refuses to move by any significant amount until the field reaches a critical value, at which point the wall passes through the corner and moves all the way to  $s = 95$ . Figure 5(a) shows the computed position of the wall center as a

function of the magnitude of the applied field. The critical field (i.e., the wall motion coercivity) is  $H_c = 3.2 \text{ kOe}$  in this case. Figure 5(b) shows the shapes of the wall at several points during this simulation. The wall basically maintains its shape, even when it is pinned down at the corner of the sidewall. The above results can be understood by energy considerations. When the wall resides far from the corner, it is easy to make it move to the right. However, close to the kink, any slight movement to the right, will increase the wall energy because of an increase in the surface area of the wall. Thus, unless the applied field is strong enough, wall motion will not occur and the domain wall will remain pinned around the corner. Figure 5(c) shows the exchange and anisotropy energies of the lattice at various wall positions. Both energies are seen to be constant when the wall is in regions with uniform thickness. In the region of varying thickness, the energies increase almost linearly with the wall position, but the two remain very close to each other at all times. Figure 6(a) shows the critical field versus the initial film thickness  $h_1$  with the value of  $\alpha$  fixed at  $45^\circ$ . Figure 6(b) shows the critical field versus the angle  $\alpha$  with the initial film thickness  $h_1$  fixed at  $150 \text{ \AA}$ . [In both cases  $h_2 = h_1 + l \cdot \tan(\alpha)$ .] Based on these simulation results, we conclude that smaller initial thickness  $h_1$  and/or larger angle  $\alpha$ , will be associated with larger values of coercivity. Roughly speaking, the initial film thickness  $h_1$  is proportional to the height of a platform from which the wall will have to jump over the energy barrier, and the gradient of the film thickness,  $\tan(\alpha)$ , is proportional to the height of the energy barrier itself. Therefore, it will be easier to release the wall from the pinning site when  $h_1$  is large or when  $\alpha$  is small.

Using theoretical arguments, we derive an expression for the coercivity of wall motion in terms of  $h_1$  and  $\alpha$  in the following subsection. In Fig. 6, the solid circles are the data points obtained by computer simulation, and the continuous curves are the theoretical estimates. When the applied field is well below the anisotropy field  $H_k = 2K_u/M_s$ , we found that the analytic results and the computer simulations agree quite well.

## C. Analytic derivation of coercivity

The cross section of a magnetic film in the vicinity of a sidewall may resemble that shown in Fig. 4. Its length  $2L$  is much greater than the width of the magnetic domain wall,  $4\delta$ . The thickness of the film is a function of  $x$ , say,  $h(x)$ . In this section, the zero point of the coordinate  $x$  is defined at the lower corner of the sidewall (in Fig. 4 this corner is located at lattice site  $s = 35$ ). In the interval  $[0, l]$  (corresponding to  $s \in [35, 65]$  in Fig. 4), thickness varies continuously with a gradient of  $\tan(\alpha)$ .  $h(x) = h_1$  for  $x < 0$ ; and  $h(x) = h_2$  for  $x > l$ . For simplicity, we will assume that the width of the film in the  $Y$  direction (perpendicular to the plane of the figure) is unity. We calculate the total energy of the lattice in terms of the domain wall position  $a$  and the applied magnetic field  $H_{\text{ext}}$ . Under the condition of the applied field being much weaker than the anisotropy field  $H_k$ , we can safely assume that the shape of the domain wall will remain intact as the wall assumes different positions under the influence of

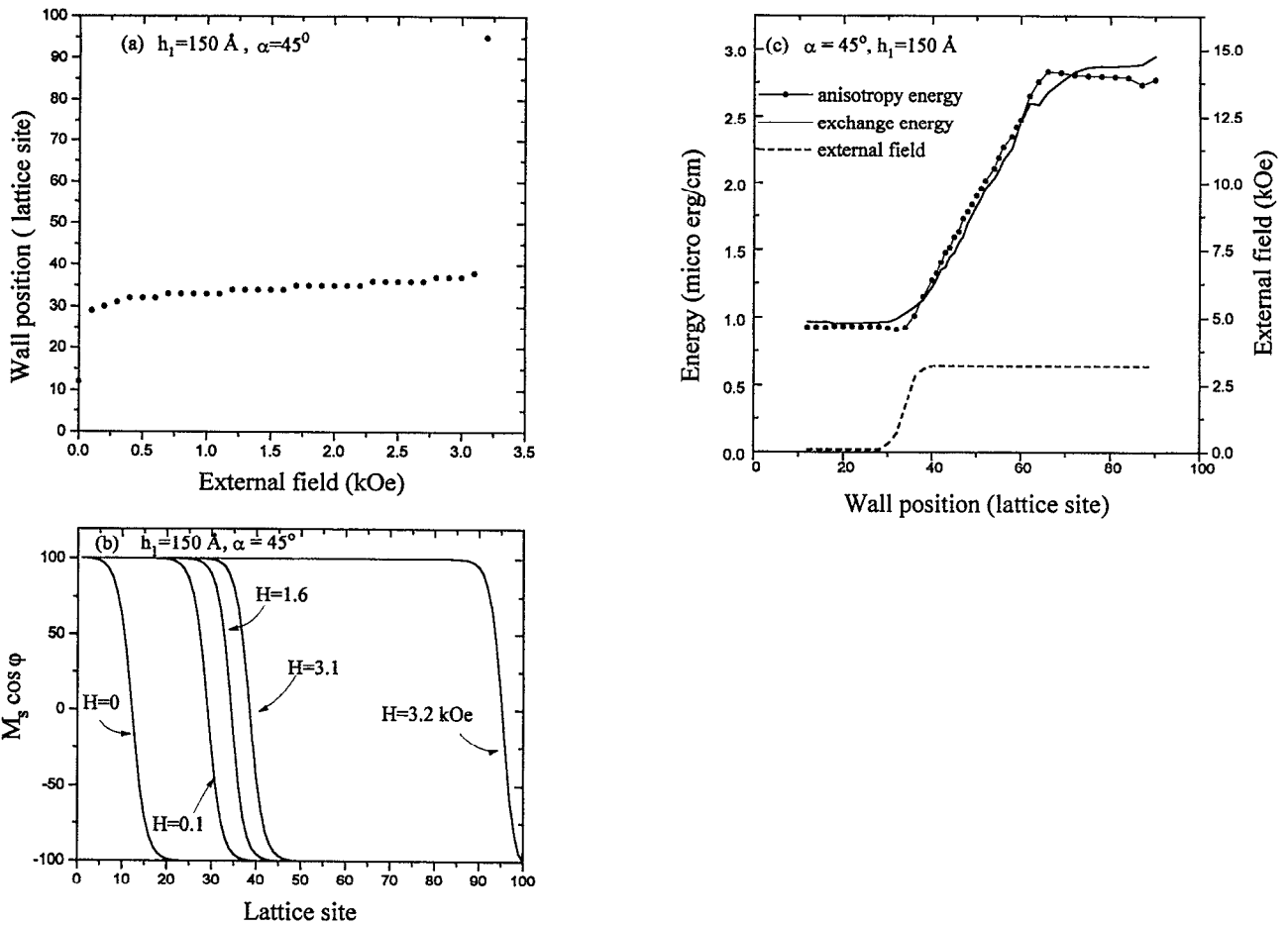


FIG. 5. (a) Computed position of the wall center as a function of the magnitude of the external field. The wall, initially placed at  $s=12$ , moves to  $s=29$  under an applied field of 0.1 kOe and stays around the corner at  $s=35$  until the field reaches 3.2 kOe. At this point, the wall overcomes sticking at the corner and moves on to the thick region of the film. Note that an applied field of 0.1 kOe cannot push the wall to the corner at  $s=35$ , but keeps it away at a distance of about half the wall width. Thus, when the wall has such a distance to the corner, it begins to feel the kink in the film thickness. (b) Distribution of the Z component of magnetization,  $M_z = M_s \cos \phi$  over the lattice of dipoles, corresponding to several values of the external field. Under different magnetic fields and in different thickness regions, the wall is seen to essentially retain its original shape. (c) Exchange and anisotropy energies of the system as functions of the wall position. When the wall is in a region of uniform thickness, its anisotropy and exchange energies are constant, but when it enters the gradient part of the film, these energies rise linearly with the film thickness.

a varying applied magnetic field. In our simulations, the applied field is always less than the anisotropy field and also much less than the exchange field. As before,  $K_u$  and  $A_x$  denote the anisotropy constant and the exchange stiffness coefficient, respectively. Without an applied field, the angle  $\phi$  of a domain wall centered at  $x=a$  can be expressed as

$$\phi(x-a) = 2 \tan^{-1} \left[ \exp \left( \frac{x-a}{\delta} \right) \right], \quad (3)$$

where  $\delta = (A_x/K_u)^{1/2}$  is the wall width parameter; the actual wall width being around  $4\delta$ . Assuming that the exchange and anisotropy energies are equal, the wall energy is going to be twice the anisotropy energy, namely,

$$\begin{aligned} E_{\text{wall}} &= 2K_u \int_{-L}^L \sin^2[\phi(x-a)]h(x)dx \\ &= 2K_u \int_{-L-a}^{L-a} \sin^2 \phi(x)h(x+a)dx. \end{aligned} \quad (4)$$

The external field energy will be

$$\begin{aligned} E_{\text{ext}} &= -H_{\text{ext}}M_s \int_{-L}^L \cos[\phi(x-a)]h(x)dx \\ &= -H_{\text{ext}}M_s \int_{-L-a}^{L-a} \cos \phi(x)h(x+a)dx. \end{aligned} \quad (5)$$

The total energy of the system is the sum of the above energies, namely,  $E_{\text{total}} = E_{\text{wall}} + E_{\text{ext}}$ . Clearly  $E_{\text{total}}$  is a function of the wall center position  $a$  and of the applied field  $H_{\text{ext}}$ .

In accordance with the minimum energy principle, the wall will move to a new position if its total energy can be lowered relative to the current position. Therefore, the sign of the derivative of  $E_{\text{total}}$  with respect to the wall position  $a$  will carry information about the direction of wall motion:

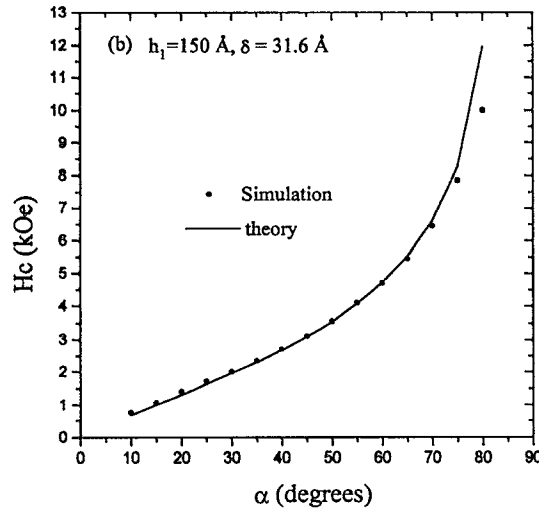
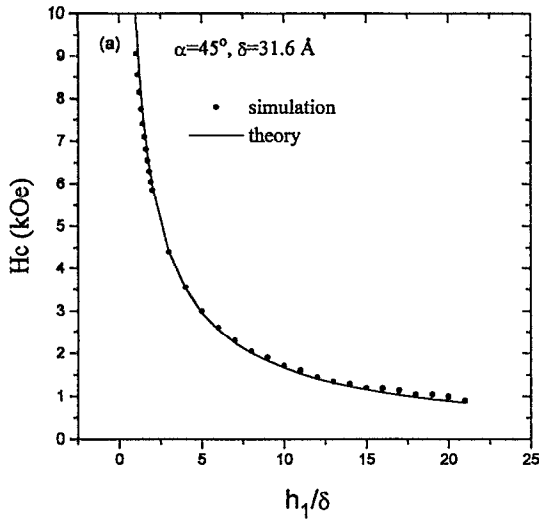


FIG. 6. (a) Computed coercivity vs the initial film thickness  $h_1$  for a corner angle of  $45^\circ$ . Note that  $h_2 = h_1 + l$ , where  $l = 300 \text{ \AA}$ . (b) Computed coercivity vs the corner angle  $\alpha$  for an initial film thickness  $h_1 = 150 \text{ \AA}$ . In general,  $h_2 = h_1 + l \cdot \tan(\alpha)$  where  $l = 300 \text{ \AA}$ . The solid circles are the points obtained by simulation, while the continuous curve is based on theory. At large angles or at small values of the initial film thickness, coercivity is large. The simulation results are very close to the theoretical estimate, mainly because the magnetic field is small compared to the anisotropy field.

$$\begin{aligned} \frac{dE_{\text{total}}}{da} = & 2K_u \left[ \sin^2[\varphi(-L-a)]h(-L) - \sin^2[\varphi(L-a)] \right. \\ & \times h(L) + \int_{-L-a}^{L-a} \sin^2 \varphi(x) \left( \frac{dh(x+a)}{da} \right) dx \left. \right] \\ & - H_{\text{ext}} M_s \left[ \cos[\varphi(-L-a)]h(-L) - \cos[\varphi(L-a)] \right. \\ & \left. - a) \right] h(L) + \int_{-L-a}^{L-a} \cos \varphi(x) \left( \frac{dh(x+a)}{da} \right) dx \left. \right]. \quad (6) \end{aligned}$$

For the sample thickness profile shown in Fig. 4, the derivative of  $h(x)$  is readily obtained as follows:

$$\frac{dh(x)}{da} = \begin{cases} \tan(\alpha) & x \in [0, l] \\ 0 & \text{otherwise.} \end{cases} \quad (7)$$

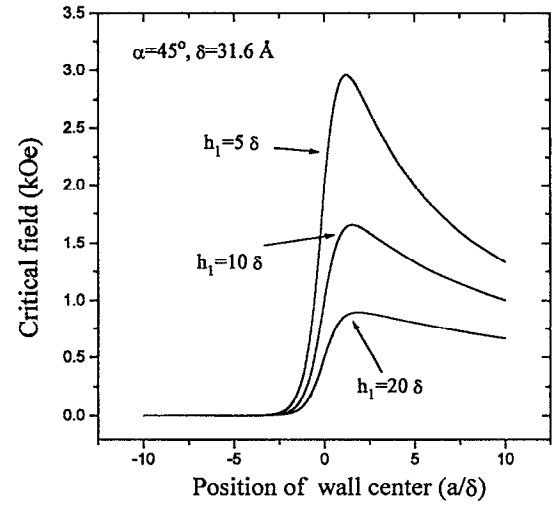


FIG. 7. Theoretical plots showing the critical field  $H_c$  as a function of position of the wall center, which is shown in Eq. (12) with initial film thickness  $h_1 = 5\delta$ ,  $10\delta$ , and  $20\delta$ . The angle  $\alpha$  is assumed to be  $45^\circ$ , and the width of the transition region from  $h_1$  to  $h_2$  is assumed to be much larger than the domain wall width. When the wall is far from the corner (i.e.,  $a \ll 0$ ), the critical field is essentially zero. However, as the wall center approaches the corner to within half of the wall width,  $2\delta$ , it begins to feel the presence of the thicker region; the critical field then rises rapidly. The maximum field always appears close to this corner, but its exact location and magnitude depend on the initial film thickness  $h_1$ . With smaller  $h_1$ , the coercivity (the maximum value of the critical field) is larger and the point at which the maximum value occurs is closer to the corner. Theoretically, when  $h_1 < \delta$ , the maximum value of the critical field will appear exactly at the corner.

When the wall center is far from the boundaries of the film, we have

$$\begin{aligned} L \gg a, \quad \varphi(-L-a) = 0, \quad \varphi(L-a) = \pi, \\ h(-L) = h_1, \quad h(L) = h_2. \end{aligned} \quad (8)$$

Equation (6) may now be written

$$\begin{aligned} \frac{dE_{\text{total}}}{da} = & 2K_u \tan(\alpha) \int_{-a}^{-a+l} \sin^2 \varphi(x) dx - H_{\text{ext}} M_s \\ & \times \left( h_1 + h_2 + \tan(\alpha) \int_{-a}^{-a+l} \cos \varphi(x) dx \right). \quad (9) \end{aligned}$$

Setting the derivative equal to zero, yields the critical field as follows:

$$\begin{aligned} H_c(a) = & \frac{2K_u \tan(\alpha) \int_{-a}^{-a+l} \sin^2 \varphi(x) dx}{M_s [h_1 + h_2 + \tan(\alpha) \int_{-a}^{-a+l} \cos \varphi(x) dx]} \\ = & \frac{2K_u}{M_s} \left[ \frac{2\delta \tan(\alpha)}{h_1 + h_2 + \tan(\alpha) \int_{-a}^{-a+l} \cos \varphi(x) dx} \right] \\ & \times \left( \frac{1}{1 + \exp[-(2a/\delta)]} - \frac{1}{1 + \exp[2(l-a)/\delta]} \right). \quad (10) \end{aligned}$$

Equation (10) gives the required field for moving the wall to the right in terms of the film's geometric and magnetic pa-

rameters. When  $a$  is far from the corner,  $H_c$  is close to zero (that is, the wall has not yet begun to feel the thickness variation). The maximum value of the critical field in Eq. (10) is the coercivity of this system. The point where  $H_c(a)$  in Eq. (10) has its maximum always appears near the kink. Below, we consider two cases.

### 1. Case 1

The length of the gradient region  $l$  is much larger than  $\delta$ . Since the position  $a$  at which  $H_c$  attains its maximum will be of the order of  $\delta$ , the second exponential term in Eq. (10) can be ignored, and the term containing  $\cos(\phi)$  can be approximated as follows:

$$\begin{aligned} \tan(\alpha) \int_{-a}^{-a+l} \cos \varphi(x) dx &\approx \tan(\alpha)(l-2a)\cos[\varphi(-a+l)] \\ &\approx \tan(\alpha)(l-2a)\cos(\pi) \\ &= 2a \tan(\alpha) - (h_2 - h_1). \end{aligned} \quad (11)$$

The critical field is thus written

$$H_c = \frac{2\sqrt{A_x K_u} \tan(\alpha)}{M_s[h_1 + a \tan(\alpha)]} \left[ \frac{1}{1 + \exp(-2a/\delta)} \right]. \quad (12)$$

Figure 7 shows the dependence of  $H_c$  on the wall center position  $a$ , as given by Eq. (12). This is also the equation that is used to obtain the continuous curves in Figs. 6(a) and 6(b).

### 2. Case 2

Consider a  $90^\circ$  corner. In this case the length  $l$  approaches zero, and  $\tan(\alpha)$  goes to infinity, but the product of these terms remains constant

$$l \rightarrow 0, \quad \alpha \rightarrow \pi/2, \quad l \tan(\alpha) \rightarrow (h_2 - h_1).$$

Under these circumstances, Eq. (10) can be written as follows:

$$\begin{aligned} H_c &= \lim_{l \rightarrow 0, \alpha \rightarrow \pi/2} \left[ \frac{2K_u \tan(\alpha)}{M_s(h_1 + h_2)} \right] \\ &\times \left\{ \frac{\exp(-2a/\delta)[\exp(2l/\delta) - 1]}{[\exp(-2a/\delta) + 1]^2} \right\} (2\delta) \\ &= \frac{2K_u}{M_s(h_1 + h_2)} \left( \frac{2}{1 + \cosh(a/\delta)} \right) \lim_{l \rightarrow 0, \alpha \rightarrow \pi/2} [l \tan(\alpha)] \\ &= \frac{2K_u(h_2 - h_1)}{M_s(h_2 + h_1)} \left( \frac{2}{1 + \cosh(a/\delta)} \right). \end{aligned} \quad (13)$$

Thus, when the wall is far from the corner, the hyperbolic term approaches zero, and a small field can push the wall to the right. The largest field is required when the wall center is at the kink itself, i.e., when  $a=0$ . To push the wall through the kink,  $H_{\text{ext}}$  must be greater than or equal to  $[2K_u(h_2 - h_1)]/[M_s(h_2 + h_1)]$ , which is proportional to the fractional step height, and is also less than the anisotropy field  $H_k = 2K_u/M_s$ .

### ACKNOWLEDGMENT

This work has been supported by the Advanced Research Projects Agency (ARPA) under Contract No. MDA-972-93-1-0009.

<sup>1</sup>K. Ichihara, J. Appl. Phys. **67**, 6552 (1990).

<sup>2</sup>S. Gadetsky, T. Suzuki, J. K. Erwin, and M. Mansuripur, IEEE Trans. Magnet. **30**, 4404 (1994).

<sup>3</sup>S. Gadetsky, T. Suzuki, J. K. Erwin, and M. Mansuripur, J. Magn. Soc. Jpn. **19** (S1), 91 (1995).

<sup>4</sup>M. Mansuripur, J. Appl. Phys. **63**, 5809 (1988).